Combined multi-wavelength laser speckle contrast imaging and diffuse reflectance imaging for skin perfusion assessment

A. Sdobnov, A. Bykov, A. Popov, I. Lihacova, A. Lihachev, et al.

A. Sdobnov, A. Bykov, A. Popov, I. Lihacova, A. Lihachev, J. Spigulis, I. Meglinski, "Combined multi-wavelength laser speckle contrast imaging and diffuse reflectance imaging for skin perfusion assessment," Proc. SPIE 11075, Novel Biophotonics Techniques and Applications V, 110751F (22 July 2019); doi: 10.1117/12.2526921

SPIE.

Event: European Conferences on Biomedical Optics, 2019, Munich, Germany

Combined Multi-Wavelength Laser Speckle Contrast Imaging and Diffuse Reflectance Imaging for Skin Perfusion Assessment

A. Sdobnov[a,*], A. Bykov[a], A. Popov[a], I. Lihacova[b], A. Lihachev[b], J. Spigulis[b], and I. Meglinski[a]

[a] University of Oulu, Optoelectronics and Measurement Techniques, Oulu, FI-90014, Finland
[b] University of Latvia, Institute of Atomic Physics and Spectroscopy, Riga, LV-1050, Latvia

ABSTRACT

Laser Speckle Contrast Imaging (LSCI) is a powerful low-cost method for visualization of flow, microcirculation and blood perfusion. Due to the fact that diseased and healthy tissues has different blood perfusion, LSCI can be a perspective tool for cancer diagnostics and discrimination between different types of tissues. Previously, multispectral diffuse reflectance imaging method for melanoma diagnostics has been introduced. In this work, multi-wavelength (532-, 655- and 850- nm) LSCI technique combined with hyperspectral camera and diffuse reflectance imaging method will be used for assessment of tissues with different skin perfusion properties. An *in vivo* experiment with occlusion in human finger was performed serving as a model of tissues with different perfusion properties. The proposed method still requires further development and improvements to become a real clinical laboratory tool for non-invasive skin cancer diagnostics.

Keywords: Speckle, hyperspectral imaging, speckle contrast, speckle imaging, skin perfusion, skin cancer

1. INTRODUCTION

The incidence of skin cancer is increasing in Europe and worldwide[1,2]. An early diagnosed skin cancer is characterized by good treatment prognosis and high 5-year survival rate (~97%)[3]. Late tumor detection is the main reason of the high mortality associated with skin cancer. The accessibility of early diagnostics is limited by several factors, such as high cost of dermatological services, long queues on state-funded oncologist examinations, as well as inaccessibility of oncologists in the countryside regions - this is an actual clinical problem. The new strategies and guidelines for skin cancer early detection and post-surgical follow-up intend to realize the Full Body Examination (FBE) by primary care physicians (general practitioners, interns) in combination with classical dermoscopy[4]. However, the effective implementation of FBE strategy is still limited by several risks that are mainly associated with subjective interpretation of the dermoscopic results leading to insufficient balance between false positive and false negative results[5]. To reduce these risks, it is necessary to equip primary care physicians with devices with the following features: low cost, compactness and portability, providing fast diagnosis results, non-invasiveness (no biopsy), high sensitivity and accuracy. Optical Coherence Tomography (OCT) has been used extensively for studies of blood flow in various vascular beds, including complex vessels and port-wine stains[6-8] .Commercial devices exploiting skin multispectral reflectance and fluorescence features such as MelaFind, SIAscope, Velscope are suitable for non-invasive cancer diagnostics. However, they face multiple problems: insufficient specificity[9,10], infrastructure requirement (Internet access) and personal data protection security risks (for remote processing-based devices). The above-mentioned technological problems are the main limiting factors of the technology wide accessibility for early diagnostics of skin cancer.

Laser Speckle Contrast Imaging (LSCI), first introduced in the early 1980s[11], is a powerful low-cost method for visualization of flow, microcirculation and blood perfusion[12-18]. As far as diseased and healthy tissues are characterized with different levels of blood perfusion[19], LSCI can be a perspective method for early diagnostics of skin cancer.

In this study, a previously developed multispectral diffuse reflectance imaging method for melanoma diagnostics[20,21] is tested using a combining multi-wavelength Laser Speckle Contrast Imaging (LSCI) technique and hyperspectral camera. An occlusion experiment in with a human finger is used for verification. Since a method developed by Diebele/Lihacova

Novel Biophotonics Techniques and Applications V, edited by Arjen Amelink, Seemantini K. Nadkarni, Proc. of SPIE-OSA
Vol. 11075, 110751F · © 2019 SPIE-OSA · CCC code: 1605-7422/19/$21 · doi: 10.1117/12.2526921

et al.[20,21] has shown a great potential for creation of an inexpensive, non-invasive device suitable for general physicians' practice, it is planned to use this method in combination with the LSCI technique for clinical applications.

2. EQUIPMENT AND METHOD

In this work, the classical LSCI scheme was used with the following improvements (see Figure 1). For multi-wavelength imaging, a hyperspectral camera has been used instead of CCD or CMOS camera. Also, a multi-wavelength light laser source was used instead of a single-wavelength source. The setup utilizes a custom-made compact light module containing a 12 mW green, a 13 mW red and a 30 mW infrared laser diodes (Roithner LaserTechnik, Austria) emitting at 532-, 650- and 850-nm wavelengths, respectively. Light beams were collimated and centered along one axis by mirror and two beam splitters (Thorlabs, USA). Emitted light was further expanded by an engineered diffuser (Thorlabs, USA) providing the uniform angular distribution of the transmitted radiation over the sample. Hyperspectral camera Nuance EX (PerknElmer, USA) was used in combination with a 60-mm F2.8 objective (Nikon, Japan) for acquisition of gray-scale raw hyper-cubes. The obtained images were further processed by custom-developed algorithm in offline regime using MATLAB r2018b software environment.

The hyperspectral camera captured hyper-cubes containing speckle images for 532-, 650- and 850-nm wavelengths at a rate of 3 frames per second, with exposure time 7 ms. For each experiment, 25 hyper-cubes were captured. Further, speckle contrast images were retrieved using spatial processing with 7x7 sq. pixels sliding window[22,23] and were averaged for each wavelength. For correct comparison between speckle contrast images at different wavelengths additional normalization on maximum value was implemented for each speckle contrast image. For this purpose, speckle contrast images from a fully static reference white object were obtained.

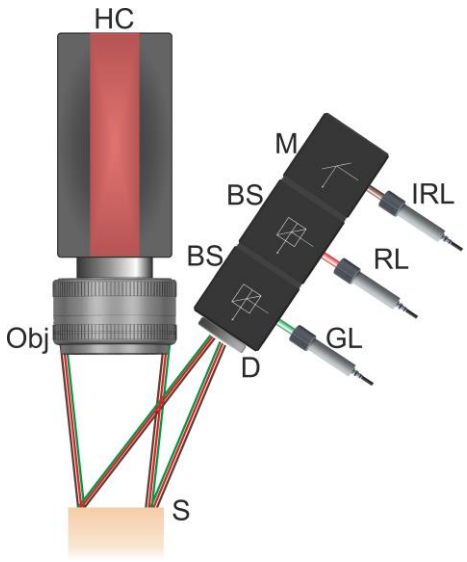

Figure 1. Schematic presentation of the multi-wavelength laser speckle contrast imaging system with a hyperspectral camera. HC – hyperspectral camera; Obj – objective; S – sample; D – diffusor; M – mirror; BS – beam splitter; IRL – infrared laser; RL – red laser; GL – green laser.

Lihacova *et al.*[20,21] introduced a parameter *p* for differentiation between melanoma and nevus. In the original work, 540-nm, 650-nm and 950-nm wavelengths were used for calculation of the parameter *p*. In our work, we used laser diodes with close wavelengths. Here, we rewrote the suggested equation from Refs. [20,21] for application with the LSCI system:

$$p = SC_{650} + SC_{850} - SC_{532}, \quad (1)$$

where SC_{532}, SC_{532} and SC_{532} are speckle contrast values at 532-nm, 650-nm and 850-nm wavelengths, respectively. The wavelength of 532 nm fits the absorption band of the blood hemoglobin[24], while at 650-nm wavelength hemoglobin absorption is minimal and melanin absorption is more pronounced[25]; 850-nm light enjoys deep penetration into the

skin[26]. The parameter *p* was calculated for each pixel of the obtained speckle contrast images. Further, the final *p* map was obtained.

3. RESULTS

As far as light with different wavelength has different penetration ability into the skin[27], use of multi-wavelength LSCI setup can be a powerful tool for detection of differences in perfusion between healthy and cancerous tissues. The possibility to obtain LSCI images at several sample depths *in vivo* was validated by monitoring occlusion in a human finger. The occlusion was induced in the middle finger of 7 healthy volunteers using a rubber band. Raw speckle images for each wavelengths were captured before the occlusion, during occlusion (3 min after start of the occlusion) and after occlusion (1 min after release of the rubber band). Such kind of experiment represents tissues with different perfusion properties.

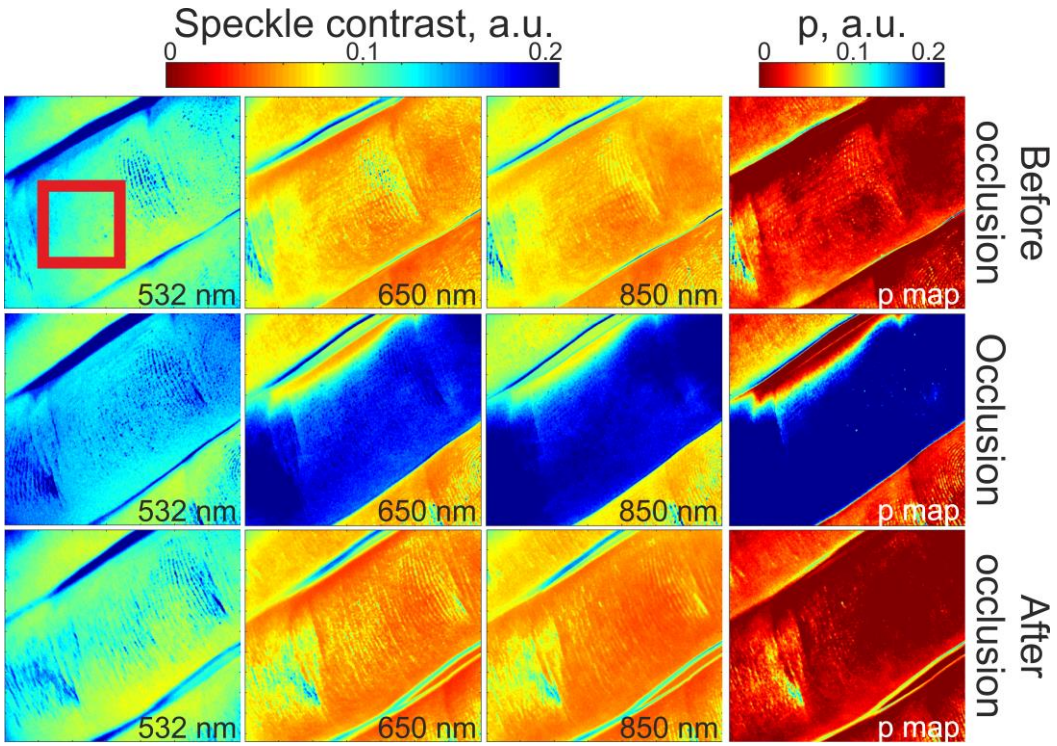

Figure 2. Laser speckle contrast images of the finger before occlusion (first row), under occlusion (second row), after occlusion (third row) at 532-, 650- and 850-nm, and the corresponding *p* map (fourth column). Red square represents the region of interest taken for average speckle contrast value calculation.

Figure 2 shows typical LSCI images obtained at 532-, 650-, 850-nm wavelength as well as a corresponding *p* map for the finger without occlusion, the finger with occlusion, and the finger after occlusion. Skin perfusion decreases during occlusion and it is clearly seen that the speckle contrast value increases for all wavelengths. In opposite, the speckle contrast value decreases for each wavelength after release of the rubber band. It can be explained by increase in skin perfusion due to active blood saturation in tissue after release of the rubber band.

Figure 3 shows averaged data of quantitative analysis for all volunteers. The error bars correspond to standard deviations. Averaged speckle contrast values inside the region of interest selected on the middle finger (the red square in Figure 2, size: 300x300 sq. pixels) were calculated at each wavelength for 7 volunteers. Figure 3(a) shows the ratio between the averaged speckle contrast value for skin during occlusion and skin before occlusion at 532-, 650-, 850-nm wavelengths. Figure 3(b) shows the ratio between the averaged speckle contrast value for skin after occlusion and skin before occlusion at 532-, 650-, 850-nm wavelengths. It is clearly seen that the greatest changes were detected at 850-nm

wavelength after occlusion compared to normal skin. This can be due to the fact that 850-nm light penetrates deeper into the skin comparing to the 532- and 650-nm wavelengths. As far as more blood arrives to the deeper skin layers, 850-nm speckle contrast images are more sensitive to the perfusion changes. Despite the fact, that changes of speckle contrast values during experiment were detected for all wavelengths, the 532-nm speckle contrast image is less sensitive to perfusion changes than 650- and 850-nm speckle contrast images. This can be explained by high absorption of 532-nm light by blood hemoglobin. It is also clearly seen that obtained *p* maps (see Figure 2) are much more sensitive to the changes in the skin perfusion than separate speckle contrast images.

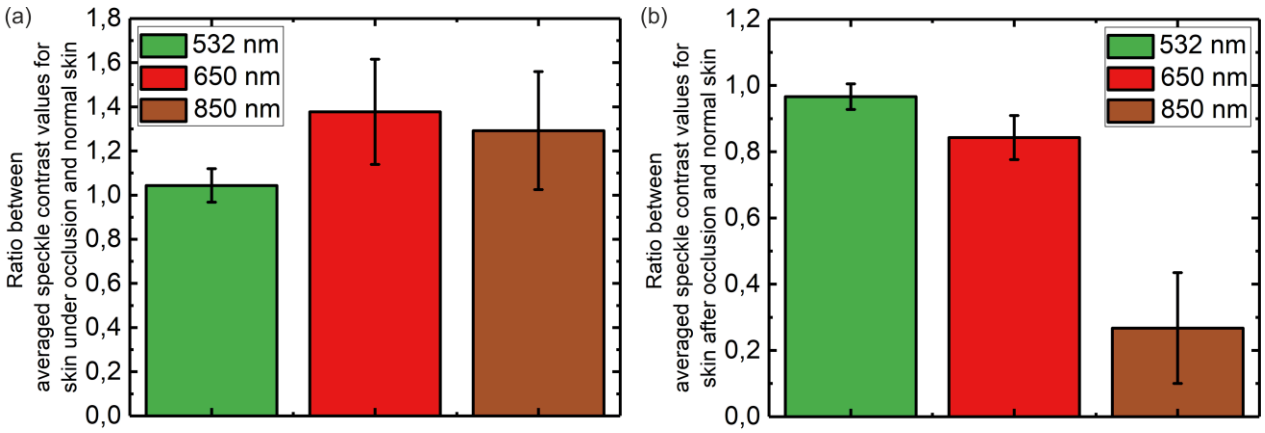

Figure 3.Ratio between averaged speckle contrast values for skin under occlusion and skin before occlusion at 532-, 650- and 850-nm wavelength (a); Ratio between averaged speckle contrast values for skin after occlusion and skin before occlusion at 532-, 650- and 850-nm wavelength (b).

Figure 4 shows averaged *p* values inside the region of interest selected on the middle finger (the red square in Figure 2, size: 300x300 sq. pixels) averaged over 7 volunteers. The red column shows the ratio between the averaged *p* value for skin during occlusion and skin before occlusion. The blue column shows the ratio between the averaged *p* value for skin after occlusion and skin before occlusion. It is clearly seen that *p* value is more sensitive to the occlusion in skin (see red column in Figure 4) than speckle contrast values for each separate wavelength. In this way, using the proposed equation based on the diffuse reflectance imaging method can be a potentially additional useful tool for advanced diagnostics of cancerous skin tissues. Also, additional application of optical clearing[28-33] can allow enhancing the penetration depth for LSCI as well as quality of the obtained data.

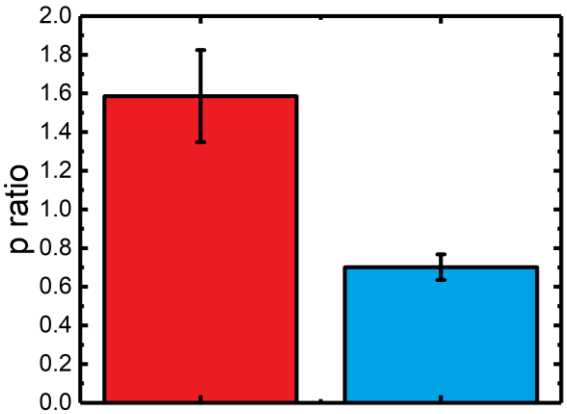

Figure 4. Ratio between averaged *p* values for skin under occlusion and skin before occlusion (red column); Ratio between averaged *p* values for skin after occlusion and skin before occlusion (blue column).

4. CONCLUSIONS

To sum up, in the current study previously developed multispectral diffuse reflectance imaging method for melanoma diagnostics has been tested using a multi-wavelength Laser Speckle Contrast Imaging (LSCI) technique combined with hyperspectral camera. To the best of our knowledge, hyperspectral camera has been used for LSCI for the first time. The *in vivo* experiment with occlusion in human finger served as a model of biotissues with different perfusion properties. Angiogenesis is the common feature that provides the growth of the tumor and it is a promoter of melanoma metastases[34]. Since with the proposed method we get a greater contrast between skin under occlusion and skin before occlusion, this application can be useful for different skin lesion classification. Furthermore, this method is easy to combine with the predetermined *p* parameter method using diffuse reflection images, thus improving diagnostic accuracy. However, for clinical implementation it is necessary to verify the described algorithm on other melanoma risk lesion groups such as nevi, pigmented basal cell carcinomas, seborrheic keratosis, and other.

5. ACKNOWLEDGMENTS

A.S was supported by Finnish Cultural Foundation (00180998). I.L. was supported by European Regional Development Fund project "Development and clinical validation of a novel cost effective multi-modal methodology for early diagnostics of skin cancers" (No. 1.1.1.2/16/I/001, agreement No. 1.1.1.2/VIAA/1/16/052). A.B. and A.P. acknowledge support provided by the Academy of Finland (290596).

REFERENCES

[1] Siegel, R.L., Miller, K.D., and Jemal, A., "Cancer statistics, 2018," CA Cancer J. Clin. 68(1), 7-30 (2018).
[2] National Cancer Institute, "Cancer Stat Facts: Melanoma of the Skin," SEER, 2018, http://seer.cancer.gov/statfacts/html/melan.html (2018).
[3] The American Cancer Society medical and editorial content team, "Melanoma survival rates," American Cancer Society, https://www.cancer.org/cancer/melanoma-skin-cancer/detection-diagnosis-staging/survival-rates-for-melanoma-skin-cancer-by-stage.html (2016).
[4] Shellenberger, R., Nabhan, M., Kakaraparthi, S., "Melanoma screening: A plan for improving early detection," Ann. Med. 48(3), 142-8 (2016).
[5] Brenner, H., "Mortality from malignant melanoma in an era of nationwide skin cancer screening," Dtsch. Arztebl. Int. 112(38), 627-8 (2015).
[6] Doronin, A., Meglinski, I., "Imaging of subcutaneous microcirculation vascular network by double correlation Optical Coherence Tomography," Las. Photon. Rev. 7(5), 797 – 800 (2013).
[7] Bonesi, M., Churmakov, D.Y., and Meglinski, I., "Study of flow dynamics in complex vessels by using Doppler Optical Coherence Tomography," Meas. Sci. Technol. 18(11), 3279-3286 (2007).
[8] Bazant-Hegemark, F., Meglinski, I., Kandamany, N., Monk, B., and Stone, N., "Optical coherence tomography: a potential tool for unsupervised prediction of treatment response for Port-Wine Stains," Photodiagnosis. Photodyn. Ther. 5(3), 191-197 (2008).
[9] Ferris, L.K., and Harris, R.J., "New diagnostic aids for melanoma," Dermatol. Clin. 30, 535–545 (2012).
[10] Ganga, R.S., Gundre, D., Bansal, S., Shirsat, P.M., Prasad, P., and Desai, R.S., "Evaluation of the diagnostic efficacy and spectrum of autofluorescence of benign, dysplastic and malignant lesions of the oral cavity using VELscope," Oral. Oncol. 75, 67–74 (2017).
[11] Fercher, A.F., and Briers, J.D., "Flow visualization by means of single-exposure speckle photography," Opt. Comm. 37(5), 326-330 (1981).
[12] Kalchenko, V., Kuznetsov, Y., Preise, D., Meglinski, I.V., and Harmelin, A. "Ear swelling test by using laser speckle imaging with a long exposure time," J. Biomed. Opt. 19(6), 060502 (2014).
[13] Meglinski, I.V., Kalchenko, V.V., Kuznetsov, Yu.L, Kuznik, B.I., and Tuchin, V.V., "Towards the nature of biological zero in the dynamic light scattering diagnostic techniques," Doklady Physics 58, 323–326 (2013).
[14] Kalchenko, V., Kuznetsov, Y., Meglinski, I. and Harmelin, A., "Label free in vivo laser speckle imaging of blood and lymph vessels," J. Biomed. Op. 17(5), 050502 (2012).
[15] Kalchenko, V., Ziv, K., Addadi, Y., Madar, N., Meglinski, I., Neeman, M. and Harmelin, A., "Combined application of dynamic light scattering imaging and fluorescence intravital microscopy in vascular biology," Laser Phys. Lett. 7(8), 603-606 (2010).

[16] Kuznetsov, Y.L., Kalchenko, V.V., Astaf'eva, N.G., and Meglinski, I.V., "Optical diagnostics of vascular reactions triggered by weak allergens using the laser speckle imaging contrast technique," Quantum Electron. 44, 713–718 (2014).
[17] Kalchenko, V., Meglinski, I., Sdobnov, A., Kuznetsov, Y.L., and Harmelin, A., "Combined laser speckle imaging and fluorescent intravital microscopy for monitoring acute vascular permeability reaction," J. Biomed. Opt. 24, (2019) // in press.
[18] Kalchenko, V., Madar, N., Meglinski, I., and Harmelin, A., "In vivo characterization of tumour and tumour vascular network using a multi-mode imaging approach," J. Biophoton. 4(9), 645–649 (2011).
[19] Ruth, B., Schmand, J., and Abendroth, D., "Noncontact determination of skin blood flow using the laser speckle method: Application to patients with peripheral arterial occlusive disease (PAOD) and to type-I diabetics," Las. Surg. Med. 13(2), 179-188 (1993).
[20] Diebele, I., Kuzmina, I., Lihachev, A., Kapostinsh, J., Derjabo, A., Valeine, L., and Spigulis, J., "Clinical evaluation of melanomas and common nevi by spectral imaging," Biomed. Opt. Express 3(3), 467-472 (2012).
[21] Lihacova, I., Bolochko, K., Plorina, E.V., Lange, M., Lihachev, A., Bliznuks, D., and Derjabo, A., "A method for skin malformation classification by combining multispectral and skin autofluorescence imaging," Proc SPIE 10685, 1068535 (2018).
[22] Sdobnov, A., Bykov, A., Molodij, G., Kalchenko, V., Jarvinen, T., Popov, A., and Meglinski, I., "Speckle dynamics under ergodicity breaking," J. Phys. D: Appl. Phys. 51(15), 155401 (2018).
[23] Sdobnov, A., Bykov, A., Popov, A., Zherebtsov, E., and Meglinski, I., "Investigation of speckle pattern dynamics by laser speckle contrast imaging," Proc. SPIE 10685, 1068509 (2018).
[24] Prahl, S., "Tabulated molar extinction coefficient for hemoglobin in water," http://omlc.ogi.edu/spectra/hemoglobin/summary.html.
[25] Sarna, T., and Swartz, H.M., "The physical properties of melanin," http://omlc.ogi.edu/spectra/melanin/eumelanin.html.
[26] Farina, B., Bartoli, C., Bono, A., Colombo, A., Lualdi, M., Tragni, G., Marchesini, R., "Multispectral imaging approach in the diagnosis of cutaneous melanoma: potentiality and limits," Phys. Med. Biol. 45(5), 1243–254 (2000).
[27] Bachem, A., and Reed, C.I., "The penetration of light through human skin," Am. J. Phys. - Leg. Cont. 97(1), 86-91 (1931).
[28] Sdobnov, A.Y., Lademann, J., Darvin, M.E., and Tuchin, V.V., "Methods for optical skin clearing in molecular optical imaging in dermatology," Biochem. (Mosc.), 84(1), 144-158 (2019).
[29] Sdobnov, A.Y., Darvin, M.E., Genina, E.A., Bashkatov, A.N., Lademann, J., and Tuchin, V.V., "Recent progress in tissue optical clearing for spectroscopic application," Spectrochim. Acta A Mol. Biomol. Spectrosc. 197, 216-229 (2018).
[30] Bykov, A., Hautala, T., Kinnunen, M., Popov, A., Karhula, S., Saarakkala, S., and Meglinski, I., "Imaging of subchondral bone by optical coherence tomography upon optical clearing of articular cartilage," J. Biophoton. 9(3), 270-275 (2016).
[31] Sdobnov, A.Y., Darvin, M.E., Schleusener, J., Lademann, J., and Tuchin, V.V., "Hydrogen bound water profiles in the skin influenced by optical clearing molecular agents—Quantitative analysis using confocal Raman microscopy," J. Biophoton. 12(5), e201800283 (2019).
[32] Sdobnov, A.Y., Tuchin, V.V., Lademann, J., and Darvin, M.E., "Confocal Raman microscopy supported by optical clearing treatment of the skin—influence on collagen hydration," J. Phys. D: Appl. Phys. 50(28), 285401 (2017).
[33] Sdobnov, A., Darvin, M.E., Lademann, J., and Tuchin, V., "A comparative study of ex vivo skin optical clearing using two-photon microscopy," J. Biophoton. 10(9), 1115-1123 (2017).
[34] Folkman, J., "Angiogenesis in cancer, vascular, rheumatoid and other disease," Nat. Med. 1, 27–30 (1995).